JP0350020

JAERI-Research
2002-034

ADSORPTION MECHANISMS AND MODELS OF ^{85}Sr, ^{237}Np, ^{238}Pu AND ^{241}Am IN LOESS MEDIA (JOINT RESEARCH)

December 2002

Tadao TANAKA, Masayuki MUKAI, Toshikatsu MAEDA
Junko MATSUMOTO, Hiromichi OGAWA, Shushen LI*
Zhiming WANG*, Jinsheng WANG*, Zede GUO* and Yingjie ZHAO*

日本原子力研究所
Japan Atomic Energy Research Institute

本レポートは，日本原子力研究所が不定期に公刊している研究報告書です。
入手の問合わせは，日本原子力研究所研究情報部研究情報課（〒319-1195　茨城県那珂郡東海村）あて，お申し越しください。なお，このほかに財団法人原子力弘済会資料センター（〒319-1195　茨城県那珂郡東海村日本原子力研究所内）で複写による実費頒布をおこなっております。

This report is issued irregularly.
Inquiries about availability of the reports should be addressed to Research Information Division, Department of Intellectual Resources, Japan Atomic Energy Research Institute, Tokai-mura, Naka-gun, Ibaraki-ken, 319-1195, Japan.

編集兼発行　　日本原子力研究所

JAERI-Research 2002-034

Adsorption Mechanisms and Models of ^{85}Sr, ^{237}Np, ^{238}Pu and ^{241}Am in Loess Media (Joint Research)

Tadao TANAKA, Masayuki MUKAI, Toshikatsu MAEDA, Junko MATSUMOTO, Hiromichi OGAWA, Shushen LI*, Zhiming WANG*, Jinsheng WANG*, Zede GUO* and Yingjie ZHAO*

Department of Fuel Cycle Safety Research
Nuclear Safety Research Center
Tokai Research Establishment
Japan Atomic Energy Research Institute,
Tokai-mura, Naka-gun, Ibaraki-ken

(Received November 5, 2002)

Adsorption mechanisms and models of ^{85}Sr(II), ^{237}Np(V), ^{238}Pu(IV) and ^{241}Am(III) on the loess were investigated from their adsorption and desorption properties. The distribution coefficient of ^{85}Sr and ^{237}Np was 2 - 3 orders of magnitude smaller than that of ^{238}Pu and ^{241}Am. The adsorption of ^{85}Sr and ^{237}Np was mainly controlled by the ion exchange reaction. On the other hand, the adsorption of ^{238}Pu and ^{241}Am was independent of the ion exchange reaction. On the basis of the experimental results, several types of adsorption models of the radionuclides, considering elemental concentrations, adsorption mechanisms and kinetics, were proposed for setting up the analytical systems of radionuclide migration in the loess media.

Keywords: Loess, Distribution coefficient, ^{85}Sr, ^{237}Np, ^{238}Pu, ^{241}Am, Adsorption, Desorption, Adsorption Mechanism, Adsorption Model.

The study was carried out under a cooperative research between Japan Atomic Energy Research Institute and China Institute for Radiation Protection.

* China Institute for Radiation Protection

^{85}Sr, ^{237}Np, ^{238}Pu 及び ^{241}Am の黄土への吸着メカニズムと吸着モデル
(共同研究)

日本原子力研究所東海研究所安全性試験研究センター燃料サイクル安全工学部
田中　忠夫・向井　雅之・前田　敏克・松本　潤子・小川　弘道
Shushen Li*・Zhiming Wang*・Jinsheng Wang*・Zede Guo*・Yingjie Zhao*

(2002 年 11 月 5 日受理)

$^{85}Sr(II)$, $^{237}Np(V)$, $^{238}Pu(IV)$ 及び $^{241}Am(III)$の黄土への吸着メカニズムと吸着モデルを吸着脱離実験結果に基づき検討した。^{85}Sr 及び ^{237}Np の分配係数は ^{238}Pu 及び ^{241}Am より２～３桁小さい値であった。分配係数が小さな^{85}Sr及び^{237}Npの黄土への吸着は，主にイオン交換によって支配されていた。一方，^{238}Pu 及び ^{241}Am の吸着メカニズムは，イオン交換に依存するものではなかった。得られた吸着脱離実験結果に基づき，黄土中における放射性核種の移行を解析する手法を確立するため，吸着の可逆性，反応速度等を考慮した吸着モデルを提案した。

本研究は，日本原子力研究所と中国輻射防護研究院との共同研究により実施された。
東海研究所：〒319-1195　茨城県那珂郡東海村白方白根 2-4
*　中国輻射防護研究院

Contents

目　次

This is a blank page.

1.Introduction

Low-level radioactive wastes containing transuranic radionuclides (TRU nuclides) such as plutonium and neptunium generated in radioactive waste treatment and in spent fuel reprocessing[1]. Since most TRU nuclides in the radioactive wastes are long-lived, they must be isolated from the biosphere for a long period of time until they are radiologic innocuous. The safety of disposal of the radioactive wastes in geological formations relies on what is known as the multi-barrier[2] concept. The geological barrier can and also must make a large contribution to the overall safety. In the geological barrier, waste components can migrate into the biosphere with circulating groundwater, accompanied with retardation by adsorption onto the geological barrier. Thus, understanding the retardation process in radionuclide migration is important in the assessment of radioactive waste disposal sites. For this purpose, JAERI and China Institute for Radiation Protection (CIRP) are studying on the migration behavior of TRU nuclides in natural environment, under the cooperative research project. In the research project, the migration test of ^{237}Np(V) and ^{238}Pu(IV) through loess media is been carrying out in the field test site of CIRP, Shanxi, China.

The retardation process can be conservatively quantified by using simple thermodynamic equilibrium: distribution coefficient (K_d) that is defined by the ratio of radionuclide concentrations on geologic media and in groundwater[3][4]. Therefore, there is a need to validate whether K_d concepts are adequate to describe the geologic media/groundwater interaction of TRU nuclides.

The aim of this work is to consider the adsorption models of TRU nuclides and the validation of the K_d concepts from the viewpoint of adsorption mechanisms of TRU nuclides in the loess media of the field test site, in order to provide the basic requirements for determining adsorption characteristics of TRU nuclides onto the loess and for setting up TRU nuclide migration models in the loess media. We have performed adsorption and desorption experiments of ^{237}Np(V), ^{238}Pu(IV) and ^{241}Am(III), which are known to be the most dominant valences in shallow geologic formations, to provide relevant adsorption data of the TRU nuclides onto the loess, and we also have elucidated adsorption mechanisms of the radionuclides by a sequential chemical extraction of the radionuclides adsorbed on the loess.

2.Experimental

2.1 Loess sample, radionuclides and solutions

The loess collected from the aerated zone of the field test site of CIRP was used in this experiment. Physico-chemical properties of the loess are presented in **Table 1**. The

loess was sieved to remove coarse particles larger than 0.5 mm.

Chlorate of $^{85}Sr^{2+}$ and nitrates of $^{237}Np(V)O_2^+$, $^{238}Pu(IV)^{4+}$ and $^{241}Am(III)^{3+}$ were used for the experiment. The ^{85}Sr was used as a reference element, since adsorption properties of it are based on a simple ion-exchange reaction, as found in previous experiments[5]. Each stock solution with radionuclide concentration of containing *ca.* 10^4 Bq/cm^3 was prepared by diluting with deionized water for ^{85}Sr, ^{237}Np, ^{238}Pu and ^{241}Am, separately. The pH of each stock solution was adjusted to *ca.* 4 with NaOH solution.

An equilibrated solution using for desorption experiments of the radionuclides adsorbed on the loess sample was prepared as follows: the loess sample amounting to 5 g had been contacted with 100 cm^3 of deionized water for 7 days. The solution was filtered using Millipore filters of 450 nm pore diameter. The solution phase separated by the filtration was used as the equilibrated solution. Chemical properties of the equilibrated solution are presented in **Table 2**

2.2 Adsorption experiments

The procedure diagram of adsorption experiment is shown in **Fig.1**. The loess sample amounting to 0.5 g had been contacted with 10 cm^3 of deionized water for 7 days. Then 0.1 cm^3 of the stock solution was added. The temperature was controlled at 25 ℃ by using an air circulation box. The solution containing the sample was gently agitated on a shaker at 60 rpm for 168 h. After the adsorption process of 0.5 − 168 h in the contact time, concentrations of ^{85}Sr, ^{237}Np and ^{241}Am in the solution were measured using an ORTEC γ -ray detector, and that of ^{238}Pu was measured using a PACKARD liquid scintillation counter, TRI-CARB 1600TR.

Distribution coefficient of the radionuclide in the adsorption process, K_d^{ads} (cm^3/g), was calculated by

$$K_d^{ads} = \frac{C_0 - C_a}{C_a} \quad \frac{V}{W}, \qquad (1)$$

where C_0 is the initial concentration of the radionuclide in solution (Bq/cm^3), C_a the concentration of the radionuclide in solution after the adsorption process (Bq/cm^3), V the volume of solution (cm^3), W the weight of loess sample (g).

A portion of the solution was sampled after the adsorption experiments for 168 h, and it was filtrated using Millipore filters of 2, 6, 20, 50, 100 and 450 nm in pore diameter. Concentrations of ^{85}Sr, ^{237}Np, ^{238}Pu or ^{241}Am in each filtrate were measured, in order to obtain particulate size distribution of the radionuclide species in the solution.

After above procedure, solution remaining in sample tube was separated from the

loess by centrifugation and was removed. The loess adsorbed the radionuclide was used for desorption experiment.

2.3 Desorption experiment

The procedure of desorption experiment is shown in **Fig.2**. Each loess sample with the radionuclide had been contacted with 10 cm^3 of the equilibrated solution for desorbing the radionuclides. After the desorption process was equilibrated under the same procedure and conditions as in the adsorption experiment. Concentrations of the radionuclide in solution were measured.

Distribution coefficient of the radionuclide in the desorption process, K_d^{des} (cm^3/g), was calculated by

$$K_d^{des} = \frac{C_0 - C_a - C_d}{C_d} \frac{V}{W}, \quad (2)$$

where C_d is the final concentration of the radionuclide in solution after the desorption process (Bq/cm^3).

Then a sequential chemical extraction of the adsorbed radionuclide was carried out to elucidate their dominant adsorption mechanisms. The first step of the extraction is the desorption of adsorbed radionuclide by using the equilibrated solution. Extracting reagents and procedures for selective extraction of the radionuclide from the samples were described as follows[5)-10)]:

Step 1: Equilibrated solution: 25 ℃, 168 h (1 time).

Step 2: 0.5 mol/dm^3 $CaCl_2$: 25 ℃, 24 h (2 times), to remove a fraction exchanged by Ca^{2+}.

Step 3: 0. 5 mol/dm^3 KCl: 25 ℃, 24 h (1 time), to remove a fraction exchanged by K^+.

Step 4: 0.1 mol/dm^3 NH_2OH-HCl + 0.1 mol/dm^3 K-oxalate: 25 ℃, 24 h (2 times), to remove a fraction adsorbed on amorphous Fe and Mn oxyhydroxide/oxide.

Step 5: 30 w% H_2O_2: 60 ℃, 3 h (1 time), to digest a fraction interacted with organic substances.

The solution extracted the radionuclide was separated from the residue by centrifugation. Radioactivities of ^{85}Sr, ^{237}Np, ^{238}Pu and ^{241}Am in each extract and radioactivities of ^{85}Sr, ^{237}Np and ^{241}Am in final residue were measured. The concentration

of ^{238}Pu remaining in the residue was estimated from the concentration of ^{238}Pu in the extract.

3. Results and discussion

3.1 Influence of contact time in the adsorption experiments

The ratio (C_a/C_0) of the radionuclide concentration at contact time t_a to the initial concentration was plotted against contact time, in **Fig.3(a)**. Apparent K_d corresponding to the concentration at each contact time t_a was calculated by Eq.(1) and is shown in **Fig.3(b)**.

The C_a/C_0 of ^{85}Sr decreased with the contact time. There were two stages in the curve of the C_a/C_0 vs. the contact time of ^{85}Sr. The C_a/C_0 of ^{85}Sr decreased rapidly in the first stage during initial 0.5 h, and apparent K_d was 32 cm^3/g. In the second stage after t_a = 0.5 h, the C_a/C_0 of ^{85}Sr was gradually decreased with contact time, and K_d value reached to 82 cm^3/g at 168 h. Most of ^{238}Pu and ^{241}Am loaded into the batch system adsorbed rapidly on the loess. More than 99 % of the ^{238}Pu and ^{241}Am were removed from the solution within 24 h, and their adsorption onto the loess was controlled by fast reactions. As to the ^{237}Np, the C_a/C_0 decreased with the contact time, about 80 % of ^{237}Np were removed from the solution after 168 h.

These results show that bulk adsorption of all four radionuclides onto the loess was controlled by fast reactions. However, considerable portion of the ^{85}Sr and ^{237}Np was controlled by slow reactions. This indicates it may be necessary to take account of kinetics into adsorption process, for the quantitative understanding in adsorption process of ^{85}Sr and ^{237}Np.

3.2 Distribution coefficients on adsorption and desorption processes

Values of distribution coefficient of the radionuclides in both adsorption and desorption processes are shown in **Table 3**. The K_d^{ads} of ^{237}Np in the adsorption process was rather small about 71 cm^3/g for the loess. The K_d^{des} of ^{237}Np in desorption process was little larger than the K_d^{ads}. The K_d^{ads} and the K_d^{des} of ^{85}Sr tended to be similar manner with those of ^{237}Np.

The K_d^{ads} of ^{238}Pu and ^{241}Am was two orders of magnitude larger than those of ^{85}Sr and ^{237}Np. The K_d^{ads} value of ^{238}Pu was 1,200 cm^3/g, and was the same value as the K_d^{des}. The K_d^{ads} and the K_d^{des} of ^{241}Am were largest among the four radionuclides, and were over 10,000 cm^3/g.

Differences between the K_d^{ads} and the K_d^{des} may reflect the adsorption mechanisms of the radionuclides.

3.3 Size distribution of the radionuclides in the solution

There are various sizes of particulate species of radionuclides in the equilibrated solution and the solutions after the adsorption experiments. Large sizes of the particulate species through geologic media might be mechanically trapped in the interstitial network, as well as adsorption. In the evaluation of the radionuclide migration, the trapped species is not regarded as a dissolved species but a species adsorbed on geologic media. Such a mechanical trap was controlled by both size of radionuclide species and interstitial diameter in geologic media.

On the assumption that the pore size of ultrafilter is the interstitial diameter in loess media, effective distribution coefficient considering the trap of the particulate species was estimated. In the present experiments, the radionuclide concentration of each filtrate could be regarded as that of dissolved species.

The effective distribution coefficient, K_d^{eff} (cm^3/g), of radionuclide between the solution and loess was calculated by the following equation:

$$K_d^{eff} = \frac{C_0 - C_e^{filter}}{C_e^{filter}} \frac{V}{W}, \quad (3)$$

where C_e^{filter} is concentration of the radionuclide in filtrate (Bq/cm^3).

The particulate size distribution of the radionuclide species in the equilibrated solution is shown in **Table 4**. No particulate ^{85}Sr and ^{237}Np was formed in the equilibrated solution. The ^{238}Pu in the equilibrated solution formed a small amount of particulate species, of which sizes were in the ranges of 2 – 6 nm and >100 nm. About 45 % of ^{241}Am in the equilibrated solution were trapped by filter of 450 nm pore diameter. The K_d^{eff} of the radionuclides is shown in **Fig.4**. The K_d^{eff} of ^{85}Sr and ^{237}Np was little affected by the size filtered. The K_d^{eff} of ^{238}Pu was little affected by the size filtered, in spite of particulate species formed in the equilibrated solution.

The mobility of particulate species through the geologic media depends on the interstitial diameter of the geologic media, so that understanding of the relationships between the particulate size and the interstitial diameter are important. The relationships might be clarified by a migration experiment of the particulate form of radionuclide.

3.4 Adsorption mechanisms of the radionuclides on the loess

Figure 5 and **Table 5** show results of the sequential chemical extraction for ^{85}Sr, ^{237}Np, ^{238}Pu and ^{241}Am adsorbed on the loess. The adsorption mechanisms of the radionuclides are discussed on the basis of the results of sequential chemical extraction.

(a) Adsorption mechanisms of ^{85}Sr

The $CaCl_2$ and KCl solutions extracted all of ^{85}Sr adsorbed on the loess. This shows almost all of the ^{85}Sr was exchanged by Ca^{2+}. Strontium and Ca belong to the same alkaline earth metal, so that the ^{85}Sr can be easily replaced with Ca^{2+} by an ion exchange reaction. Thus the adsorption of ^{85}Sr on the loess was dominated by reversible ion exchange reaction.

As shown in Table 1, calcite, which includes calcium, is major component in the loess. Furthermore high concentration of Ca^{2+} was detected in the equilibrated solution, as shown in Table 2. Small K_d of ^{85}Sr in Table 3 was probably caused by Ca containing in the loess media.

The fact that the K_d of ^{85}Sr on both the adsorption and desorption process were closed and the ^{85}Sr was adsorbed on the loess by reversible ion-exchange reaction, is expected that the migration of ^{85}Sr through the loess media must be well expressed by the conventional equilibrium adsorption model using the distribution coefficient.

(b) Adsorption mechanisms of ^{237}Np

About 53 % of ^{237}Np adsorbed on the loess were extracted with the equilibrated solution and $CaCl_2$ solution, and about 25 % of it was extracted with NH_2OH-HCl + K-oxalate or H_2O_2 solutions. This revealed that the adsorption of ^{237}Np was mainly controlled by reversible ion exchange reaction but significant portion of the ^{237}Np was tightly adsorbed as selective chemical association with Fe and/or Mn oxyhydroxide/oxide and organic substances[8][11].

The $^{237}NpO_2^+$ is the stable cationic form of neptunium in aerobic environment of generic shallow geological formations[12]. The effective charge density of this large ion is lower than that of $^{237}Np^{4+}$ produced in reduction conditions, $^{238}Pu^{4+}$ and $^{241}Am^{3+}$. Furthermore the adsorption of ^{237}Np is controlled by an ion exchange reaction, so that it must be strongly affected by coexistent cations in solution, such as H^+, Na^+ and Ca^{2+}, due to competition in adsorption between ^{237}Np and coexistent cations. Thus the distribution coefficient values of ^{237}Np were smaller than those of ^{238}Pu and ^{241}Am, as shown in Table 3.

Figure 5 shows that significant portion of ^{237}Np adsorbed on the loess reacts tightly. Kozai *et al.* reported that $^{237}NpO_2^+$ is specifically fixed in interlayer of a clay mineral like smectite[13]. The $^{237}NpO_2^+$ forms $^{237}NpO_2OH$ in alkaline solution. The $^{237}NpO_2OH$ is formed even in the equilibrated solution of pH 8.2 (Table 2). Resulting $^{237}NpO_2OH$ is able to complex with OH groups on the loess surface[14][15]. The $^{237}NpO_2^+$ adsorbed onto some minerals containing Fe(II) and Mn(II), which are contained in the loess, can be reduced into $^{237}Np^{4+}$ on solution/mineral interface, by a surface-mediated redox process[16]. Resulting $^{237}Np^{4+}$ might interact with the samples stronger than $^{237}NpO_2^+$. The non-extractable

adsorption of ^{237}Np may be caused from the specific fixation, the surface complex formation and the reduction process of $^{237}NpO_2^+$.

The results obtained in this study show that the adsorption mechanism of ^{237}Np is mainly controlled by an ion exchange reaction of $^{237}NpO_2^+$. Thus the migration of ^{237}Np in shallow geological formations may be roughly estimated by using the distribution coefficient.

(c) Adsorption mechanisms of ^{238}Pu

The adsorbed ^{238}Pu was little extracted with the equilibrated, $CaCl_2$ and KCl solutions. On the other hand, 15 % of the ^{238}Pu were extracted with NH_2OH-HCl + K-oxalate, and 70 % of it were not removed by all the extraction procedures. These results show that the adsorbed ^{238}Pu were not controlled by reversible ion exchange reaction, but by a selective chemical adsorption onto Fe and Mn oxyhydroxide/oxide and fixation. Thus ^{238}Pu can be fixed on the loess in natural environment, because also Fe and Mn oxyhydroxide/oxide does not easily dissolve in groundwater.

The authors have found that the fixation fraction, which was not removed by all the extraction procedures in Fig.5, is considered to be caused from interactions with the crystal Fe/Mn oxides and with the stable humic substance binding to the crystal Fe/Mn oxides[11]. On the other hand, valence of ^{238}Pu might vary by the surface-mediated redox process, in the same manner as the case of ^{237}Np. The changes of valence possibly affect on chemical forms and adsorption affinity of ^{238}Pu to Fe/Mn oxides[17].

Since the ^{238}Pu is combined with the loess on the basis of various reactions with Fe and Mn oxyhydroxide/oxide and humic substances, the adsorption of ^{238}Pu on the loess may be necessary to express on the basis of irreversible reactions.

(d) Adsorption mechanisms of ^{241}Am

The ^{241}Am adsorbed on the loess was little extracted with the equilibrated, $CaCl_2$, KCl and NH_2OH-HCl + K-oxalate solutions, while 12 % of it were extracted with H_2O_2 solutions. More than 80 % of the adsorbed ^{241}Am remained after all the extraction procedures. These findings indicate that the adsorption mechanisms of ^{241}Am were based on non-extractable tight reactions.

The authors have investigated relationships between the content of Fe + Mn oxides in several kinds of sedimentary samples and the irreversibly adsorbed ^{241}Am fraction, which is defined as the sum of percentage of the radionuclides extracted with NH_2OH-HCl + K-oxalate and H_2O_2 solutions, and in the final residues. And they have found that the irreversibly adsorbed ^{241}Am fraction increases with increasing Fe + Mn oxides content in the samples[11].

The distribution coefficient of ^{241}Am is largest among the four radionuclides.

Americium, present in a shallow geological environment as stable trivalent element[12], forms various complexes even in extremely low concentration region of OH^-, HCO_3^- [18][19], humic substance, so on[20][21]. Such high reactabilities of $^{241}Am(III)$ may be caused large distribution coefficient.

3.5 Influence of concentration on adsorption properties of ^{237}Np

Specific activity of ^{237}Np is very low, due to a long half life. Hence the concentration of ^{237}Np applying in the present experiments is in about 10^{-9} - 10^{-5} mol/dm^3, much higher than the other nuclides. In higher concentration range, the adsorption isotherm of ^{237}Np may be not based on Henry's type. If so, the adsorption properties of ^{237}Np on the loess are affected by its concentration.

The relationship between ^{237}Np concentration and apparent distribution coefficient K_d' corresponding to the ^{237}Np concentration is shown in **Fig.6**. The K_d' values decreased with increasing ^{237}Np concentration. **Figure 7** shows the adsorption isotherm of ^{237}Np on the loess. Plot of lnQ_a versus lnC_a was in a linear relation; Q_a is the concentration of the radionuclide adsorbed on the loess. This result indicates that the adsorption isotherm of ^{237}Np is based on Freundlich's type:

$$Q_a = aC_a^{1/n}. \quad (1<n<10) \tag{4}$$

Hence,

$$K_d' = aC_a^{(1-n)/n}, \tag{5}$$

where a and n are constant.

Thus relationship between ^{237}Np concentration and K_d' is given by $K_d' = 4\times10^2\ C_a^{-0.42}$, $K_d' = 3\times10^4\ Q_a^{-0.72}$.

In the migration test of ^{237}Np, such as column experiments and field test, the ^{237}Np concentration is expected to vary in wide ranges during the test period. In such cases, it is necessary to take account of the influence of ^{237}Np concentration into the evaluation of ^{237}Np migration.

4.Proposal of Adsorption Models

Radionuclide migration process is controlled by both flow characteristics in soil and interaction of radionuclide with geologic media[3]. The conservation of mass accompanying with water flow in geologic media can be described by

$$\frac{\partial C}{\partial t} + \frac{\rho}{\theta}\frac{\partial Q}{\partial t} = D\frac{\partial^2 C}{\partial X^2} - u\frac{\partial C}{\partial X}, \tag{6}$$

where C is radionuclide concentration in water (Bq/cm^3), Q concentration of radionuclide adsorbed on geologic media (Bq/g), ρ density of geologic media (g/cm^3), θ water content, D dispersion coefficient (cm^2/min), u velocity of water (cm/min), t time (min), and X length (cm).

On the assumption that an adsorption of radionuclide onto geologic media is based on Henry's type adsorption isotherm and equilibrium of the adsorption is attained instantaneously, the interaction is described by using the distribution coefficient K_d:

$$Q = K_d C. \tag{7}$$

The equilibrium adsorption model using K_d has been applied in some migration analysis for a long time, taking advantage of its mathematical simplicity. The adsorption models except K_d model for ^{85}Sr, ^{237}Np, ^{238}Pu and ^{241}Am were discussed, on the basis of the experimental results.

(a) Adsorption models of ^{85}Sr

The adsorption of ^{85}Sr tended to be dependent on reaction time, since the C_a/C_0 reduced with contact time, as shown in Fig.3(a). In the consideration of reaction rates in the adsorption and desorption processes, the adsorption model can be expressed by[22]

$$\frac{\partial Q}{\partial t} = k_1 C - k_2 Q, \tag{8}$$

where k_1 is rate constant of adsorption (cm^3/g/h) and k_2 is rate constant of desorption (1/h).

The relationship between C_a/C_0 and contact time, as shown in Fig.3(a), indicated that the adsorption of ^{85}Sr was consisted of two processes; one was finished immediately and another was proceeded gradually. The fact that there are both the immediate and gradual processes induces to apply a reversible non-equilibrium adsorption model, considering both equilibrium and kinetic in the adsorption process[23]:

$$Q_1 = K_{d0} C \tag{9}$$

$$\frac{\partial Q_2}{\partial t} = k_1 C - k_2 Q_2 \tag{10}$$

$$Q = Q_1 + Q_2, \tag{11}$$

where Q_1 is concentration of radionuclide adsorbed in the instantaneous equilibrium process (Bq/g), Q_2 concentration of radionuclide adsorbed in the kinetic process (Bq/g), and K_{d0} distribution coefficient corresponding to the instantaneous equilibrium (cm^3/g).

Hence,

$$\frac{\partial Q}{\partial t} = K_{d0}\frac{\partial C}{\partial t} + k_1 C - k_2(Q - K_{d0}C). \tag{12}$$

(b) Adsorption models of ^{237}Np

Since the adsorption of ^{237}Np is not based on Henry's type adsorption isotherm, the adsorption model cannot be expressed by a constant K_d value, even on the assumption that the adsorption equilibrium is attained instantaneously. The adsorption is described as a function of the radionuclide concentration in solution:

$$Q = aC^{1/n}. \tag{13}$$

On the other hand, a portion of specific ^{237}Np species may irreversibly adsorb on the loess, as shown in Fig.5. Provided the ^{237}Np species irreversibly adsorbs onto the loess with reaction rate k_1, the adsorption of ^{237}Np can be explained by introducing[24]

$$Q_3 = aC_3^{1/n} \tag{14}$$

$$\frac{\partial Q_4}{\partial t} = k_1 C_4 \tag{15}$$

$$C = C_3 + C_4,\ Q = Q_3 + Q_4, \tag{16}$$

where C_3 is concentration of ^{237}Np species relating to reversible adsorption in the solution and Q_3 is concentration of that adsorbed on the loess, and C_4, is concentration of ^{237}Np species relating to irreversible adsorption in the solution and Q_4 is concentration of that adsorbed on the loess.

The adsorption of ^{237}Np is dependent on the reaction time, in the similar manner as that of ^{85}Sr adsorption, as shown in Fig.3(a). In such a case, the adsorption model of ^{237}Np is given by Eq.(8).

(c) Adsorption models of ^{238}Pu

The adsorption mechanism of ^{238}Pu on the loess is apparently dominated with the irreversible reaction. Thus the adsorption model can be described by

$$\frac{\partial Q}{\partial t} = k_1 C. \tag{17}$$

If apparent irreversible adsorption of ^{238}Pu is attributable to extremely small k_2 as compared to k_1, the adsorption of ^{238}Pu can be explained by introducing

$$\frac{\partial Q}{\partial t} = k_1 C - k_2 Q. \quad (k_1 >> k_2) \tag{18}$$

On the other hand, a portion of ^{238}Pu may reversibly adsorb on the loess. Provided the ^{238}Pu species adsorbs reversibly and instantaneously onto the loess, the adsorption of ^{238}Pu can be expressed by

$$Q_1 = K_d C_1 \tag{19}$$

$$\frac{\partial Q_2}{\partial t} = k_1 C_2 \tag{20}$$

$$C = C_1 + C_2,\ Q = Q_1 + Q_2 . \qquad (C_1 << C_2,\ Q_1 << Q_2) \tag{21}$$

(d) Adsorption models of ^{241}Am

The ^{241}Am formed particulate species in the equilibrated solution and the adsorption mechanisms of ^{241}Am on the loess were apparently dominated by the irreversible reaction. Thus the migration of ^{241}Am through the loess media may not be explained by the K_d concept based on instantaneous equilibrium. In the case that the adsorption is based on the irreversible reaction, the adsorption of ^{241}Am can be described by Eq.(17).

Provided the particulate ^{241}Am species can pass through interstitial matrix, the adsorption of such particulate species may be expressed by the K_d concept Eq.(7)[25][26]. On the other hand, in the case that the particulate is trapped by interstitial matrix, an equation based on filtration theory was proposed to evaluate the migration of particulate ^{241}Am. The filtration formula[27] is generally expressed by

$$\frac{\partial C_p}{\partial X} = -\lambda C_p , \tag{22}$$

where λ is filtration factor (1/cm) and C_p is concentration of particulate in solution passed through soil layer of X cm.

Solving Eq.(22) for $C_p = C_{p0}$ ($X = 0$) and constant C_{p0}, we obtain

$$\frac{C_p}{C_{p0}} = \exp(-\lambda X), \tag{23}$$

Hence, the particulate concentration at any position in geologic media is given by the equation

$$\frac{Q_p}{Q_{p0}} = \exp(-\lambda X_j), \tag{24}$$

where Q_p is particulate concentration detained at X_j of soil layer (Bq/g) and Q_{p0} is particulate concentration detained at influent edge of geologic media (Bq/g).

Values of C_p and Q_p can be obtained as a function of λ and X.

5.Conclusions

The distribution coefficient of ^{85}Sr and ^{237}Np was 2 - 3 orders of magnitude smaller than that of ^{238}Pu and ^{241}Am, and the reaction rate of them was partially controlled by slow reactions. The adsorption of ^{85}Sr and ^{237}Np, which are cationic form in the solution, was mainly controlled by the ion exchange reaction. On the other hand, the adsorption of ^{238}Pu and ^{241}Am, a portion of which forms particulate species in the solution, was independent of the ion exchange reaction.

The adsorption mechanisms of ^{85}Sr(II), ^{237}Np(V), ^{238}Pu(IV) and ^{241}Am(III) for the loess were full of various. Several types of adsorption models of the radionuclides, considering elemental concentrations, adsorption mechanisms and kinetics, were proposed for setting up the analytical systems of radionuclide migration in the loess media, as follows. The migration of ^{85}Sr through the loess media must be well expressed by the hybrid adsorption model, considering both equilibrium and kinetic in the adsorption process. The migration of ^{237}Np and ^{238}Pu was possibly described by both the reversible and the irreversible adsorption models, corresponding to individual radionuclide species. To evaluate the migration of ^{241}Am, the adsorption model based on filtration theory of particulate

^{241}Am species was proposed.

Applicability of proposed adsorption models into the evaluation of radionuclide migration will be confirmed by analyses of the result obtained from the radionuclide migration test, performing in the CIRP's field test site.

Acknowledgements

The authors wish to express their appreciation to Dr. S.Fujine and Dr. T.Banba, Department of Fuel Cycle Safety Research, Japan Atomic Energy Research Institute, for valuable discussions.

References

(1) R.Dayal, R.F.Pietzak, J.H.Clinton: Nucl.Technol., **72**, 158 (1986).
(2) D.G.Brookins: "*Geochemical aspects of radioactive waste disposal*", Springer-Verlag, New York, 39 (1984).
(3) Y.Inoue, W.J.Kaufman: Health Phys., **9**, 705 (1963).
(4) H.M.Selim, J.M.Davidson, P.S.C.Rao: Soil Sci.Soc.Am.J., **41**, 3 (1977).
(5) T.Tanaka, *et al.*: JAERI-M 94-077, (1994).
(6) T.Tanaka, K.Sriyotha, H.Kamiyama: "*Proc. 3rd Int.Conf. on Nuclear Fuel Reprocessing and Waste Management (RECOD'91)*", Sendai, Japan, 1011 (1991).
(7) J.L.Means, D.A.Crerar, M.P.Borcsik: Geochim.Cosmochim.Acta, **42**, 1763 (1978).
(8) T.T.Chao: Soil Sci.Soc.Amer.Proc., **36**, 764 (1972).
(9) U.Schwertmann: Can.J.Soil Sci., **53**, 244 (1973).
(10) A.Tessier, P.G.C.Campbell, M.Bisson: Anal.Chem., **51**, 844 (1979).
(11) T.Tanaka, S.Muraoka: J.Radioanal.Nucl.Chem., **240**, 177 (1999).
(12) S.Nakayama: J.At.Energy Soc.J., **32**, 970 (1990).
(13) N.Kozai, T.Ohnuki, S.Muraoka: J.Nucl.Sci.Technol., **30**, 1153 (1993).
(14) Y.Sakamoto: Radioactive Waste Reserch, **1**, 107 (1994).
(15) V.Moulin, P.Robouch, P.Vitorge and B.Allard: Radiochim.Acta, **44/45**, 33 (1988).
(16) J.G.Dillard, D.L.Crowther: Geochim.Cosmochim.Acta, **48**, 1565 (1984).
(17) A.L.Sanchez, J.W.Murray, T.H.Sibley: Geochim.Cosmochim.Acta, **49**, 2297 (1985).
(18) J.I.Kim, G.Buckau, E.Bryant and R.Klenze: *ibid.*, **48**, 135 (1985).
(19) T.Yamaguchi, S.Nakayama: J.Nucl.Fuel Cycle and Environment, **3**, 49 (1996).
(20) T.Tanaka, M.Senoo: "*Scientific Basis for Nuclear Waste Management XVIII*", Materials

Research Society, Pennsylvania, 1013 (1995).
(21) H.Nitsche, E.M.Standifer: Radiochim.Acta, **46**, 185 (1989).
(22) H.Ogawa: J.Nucl.Sci.Technol., **25**, 283 (1988).
(23) T.Tanaka, *et al.*: "Proceedings of Asia Congress on Radiation Protection", Beijing, China, 681 (1993).
(24) H.Ogawa: J.At.Energy Soc.Jpn., (in Japanese), **32**, 813 (1990).
(25) T.Ohnuki, Y.Wadachi: J.At.Energy Soc.Jpn., (in Japanese), **25**, 486 (1983).
(26) H.Chinju, *et al.*: J.Nucl.Fuel Cycle and Environment, **5**, 59 (1998).
(27) Kagaku-Kougaku Kyoukai: *Roka Gizyutsu*, (in Japanese), Maki-Syoten, Tokyo, 24 (1984).

Table 1 Physico-chemical properties of the loess; The loess collected from the aerated zone of the field test site of China Institute for Radiation Protection, Shanxi, China.

Density (g/cm^3)	2.64-2.74	Permeability (10^{-4} cm/s)	1.2-2.1
Porosity (%)	45.3-53.0	Chemical composition (%)	
CEC (meq/100g)	11.7-21.3	SiO_2	58.2-66.0
Mineral composition (%)		Al_2O_3	10.9-11.5
Quartz	20-30	TiO_2	0.63-0.70
Plagioclase	15-30	Fe_2O_3	3.0-3.6
K-feldspar	10-20	CaO	7.5-9.1
Calcite	5-13	MgO	1.6-2.1
Hornblende	1-2	Na_2O	2.0-2.3
Biotite	1-4	K_2O	1.6-2.2
Chlorite	5-10	FeO	1.0-1.4

Table 2 Chemical properties of equilibrated solutions.

pH	8.1-8.4	Eh (mV)	200-400
K^+ (mg/dm^3)	0.4-5.0	$CO_3^{2-}+HCO_3^-$ ($CaCO_3$ mg/dm^3)	
Na^+ (mg/dm^3)	65-110		110-140
Mg^{2+} (mg/dm^3)	1-5	Cl^- (mg/dm^3)	24-52
Ca^{2+} (mg/dm^3)	18-25	Sr (mg/dm^3)	0.58-6.6

Concentrations of K^+, Na^+, $CO_3^{2-}+HCO_3^-$, Cl^- and Sr were determined by those of the groundwater taken from the field test site.

Table 3 Distribution coefficients of the radionuclides in both adsorption (K_d^{ads}) and desorption (K_d^{des}) processes.

	Distribution coefficient (cm^3/g)			
	^{85}Sr	^{237}Np	^{238}Pu	^{241}Am
K_d^{ads}	130	71	1200	>10000
K_d^{ads} (after 450 nm filtration)	130	78	1400	>10000
K_d^{des}	160	110	1200	>10000

Table 4 Size distribution of particulate radionuclide species in the equilibrated solution; The equilibrated solution was prepared by contacting the loess sample of 5 g with 100 cm^3 of deionized water for 7 days.

Particulate size (nm)	^{85}Sr	^{237}Np	^{238}Pu	^{241}Am
>450	0.0 %	10.1 %	20.4 %	44.8 %
100 -450	0.0 %	1.6 %	9.9 %	27.4 %
50-100	0.0 %	0.0 %	0.6 %	0.0 %
20- 50	0.0 %	0.0 %	0.2 %	0.2 %
6-20	0.0 %	0.0 %	0.2 %	0.0 %
2-6	0.0 %	7.8 %	9.1 %	25.5 %
<2	100.0 %	80.5 %	59.6 %	2.1 %

Table 5 Fraction percent of radionuclides extracted by the sequential chemical extraction technique; The extracting reagents were the equilibrated solution, 0.5 mol/dm^3 $CaCl_2$, 0. 5 mol/dm^3 KCl, 0.1 mol/dm^3 NH_2OH-HCl + 0.1 mol/dm^3 K-oxalate, and 30 w% H_2O_2.

	Percent (%)			
Extracting reagent	^{85}Sr	^{237}Np	^{238}Pu	^{241}Am
Equilibrated solution	11.2	20.5	1.7	3.1
$CaCl_2$	87.8	32.7	8.8	1.6
KCl	1.0	2.8	1.0	0.4
$NH_2OH \cdot HCl$ K-oxalate	0.0	23.7	14.9	0.8
H_2O_2	0.0	1.8	5.0	11.7
Residue	0.0	18.5	68.6	82.4

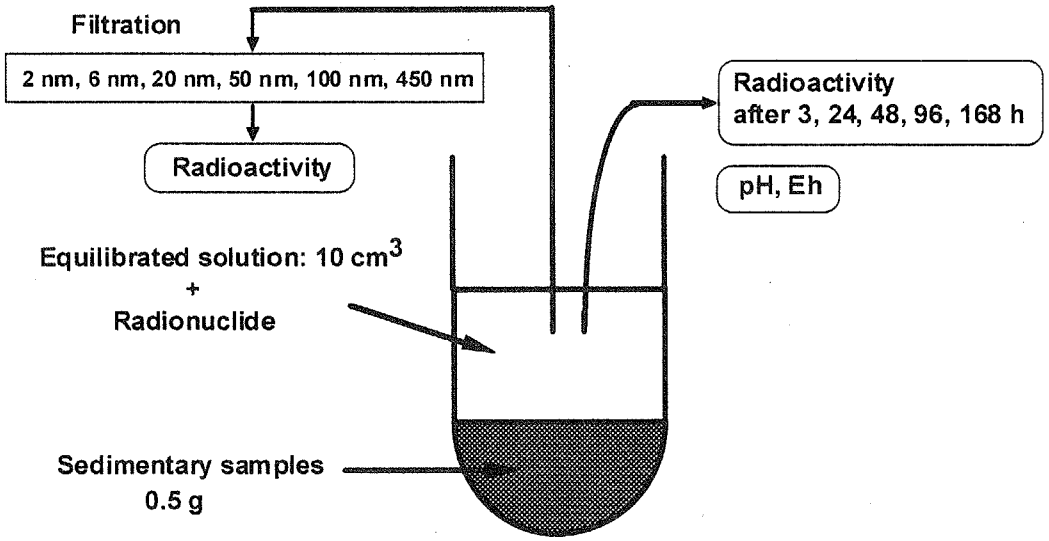

Fig.1 Procedure diagram of adsorption experiment.

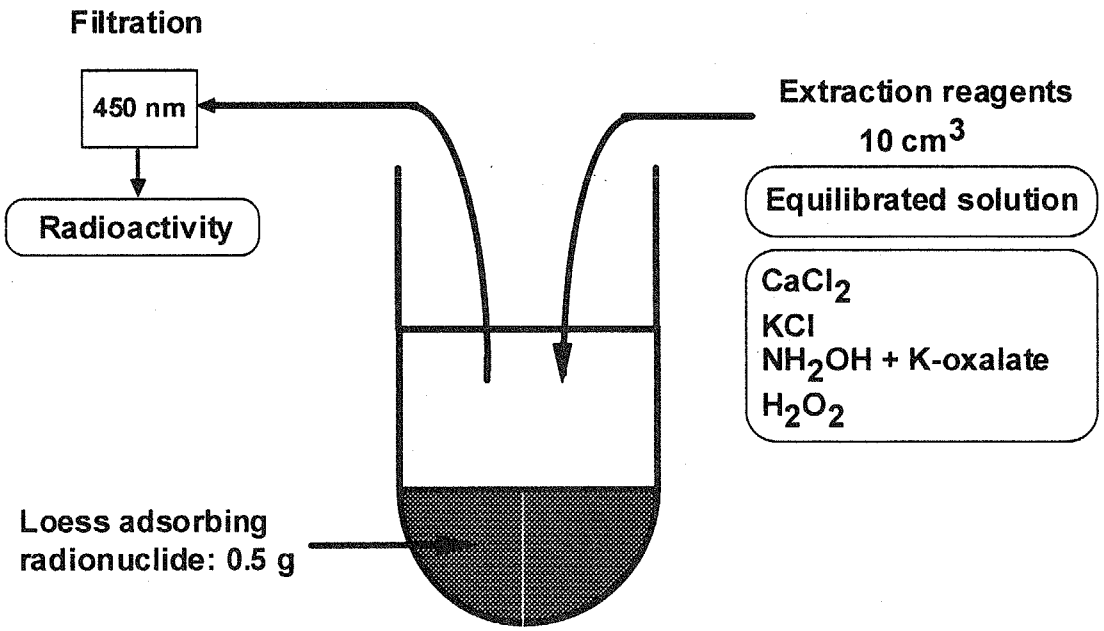

Fig.2 Procedure diagram of desorption experiment.

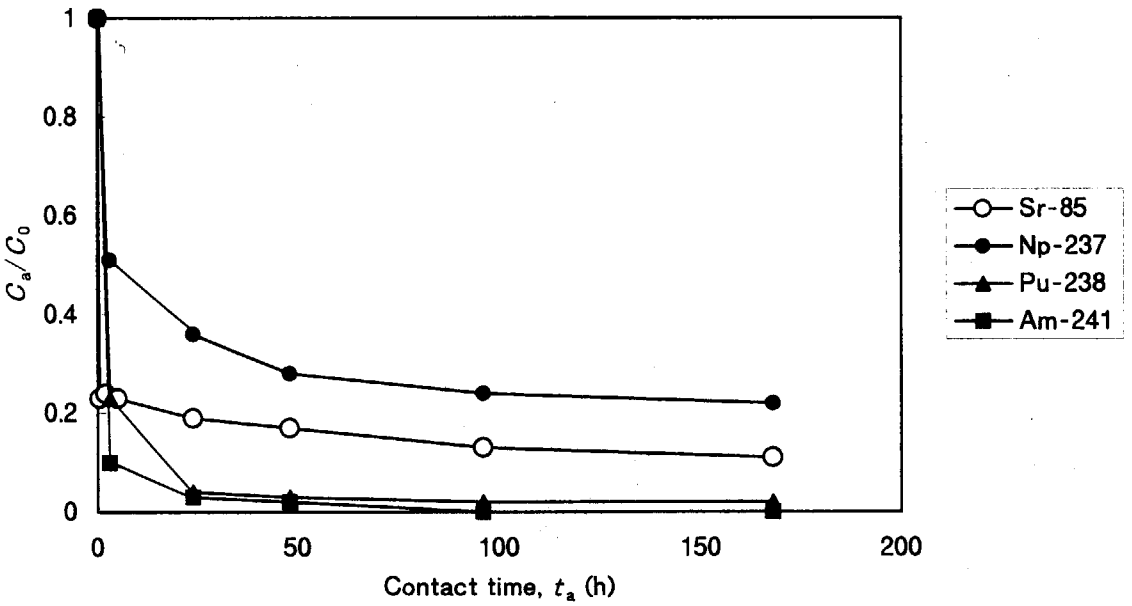

Fig.3(a) Plot of the ratio (C_a/C_0) of the radionuclide concentration at contact time t_a to the initial concentration vs. contact time.

C_a: the radionuclide concentration in solution (Bq/cm^3)

C_0: the initial concentration of the radionuclide (Bq/cm^3)

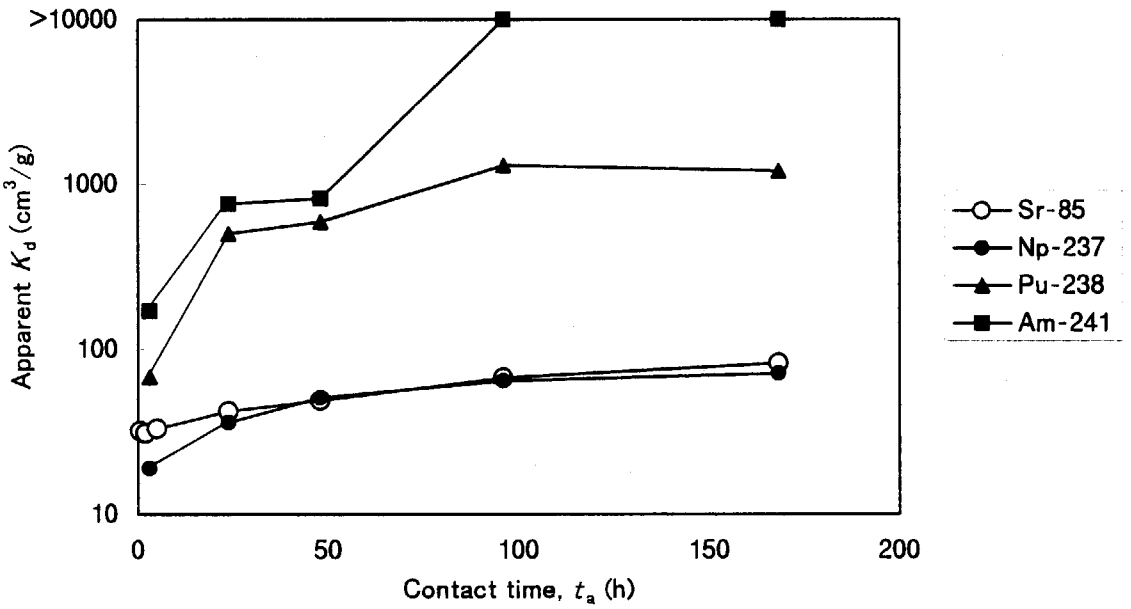

Fig.3(b) Apparent K_d corresponding to the radionuclide concentration C_a at each contact time t_a in Fig.3(a).

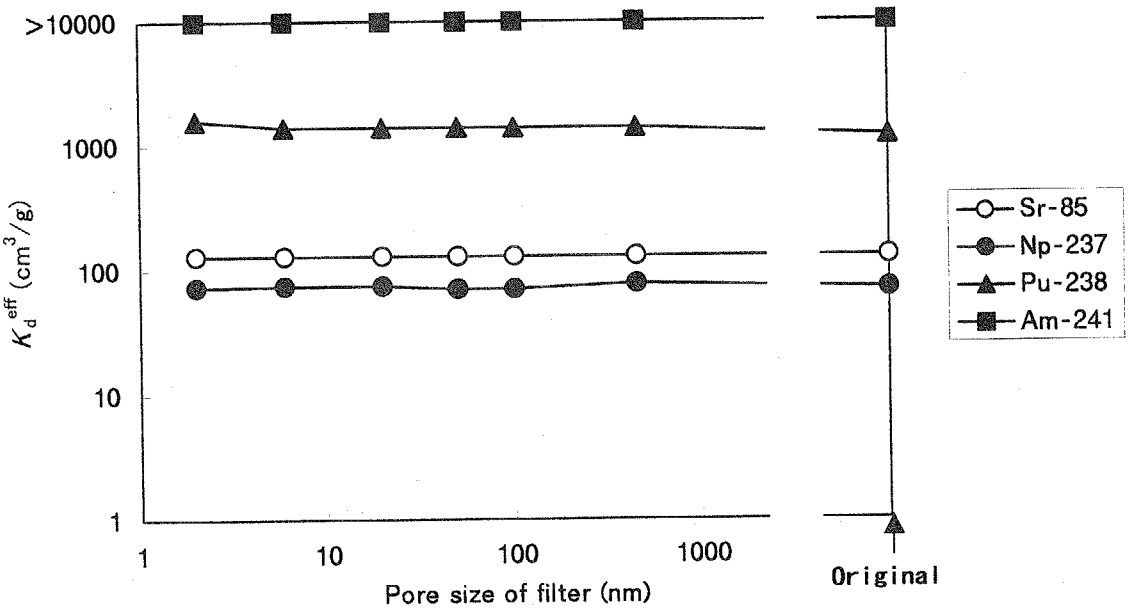

Fig.4 The effective distribution coefficient K_d^{eff}, considering the trap of the particulate species by the loess matrix, was calculated from the radionuclide concentration in each filtrate.

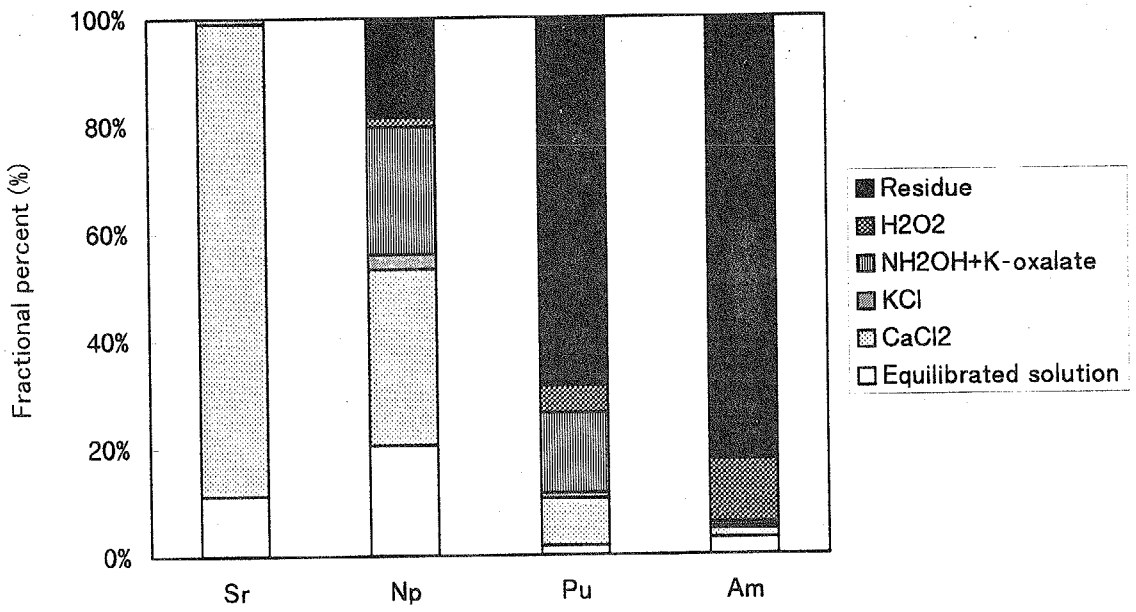

Fig.5 Percentage of ^{85}Sr, ^{237}Np, ^{238}Pu and ^{241}Am desorbed from the loess by the sequential chemical extraction technique.

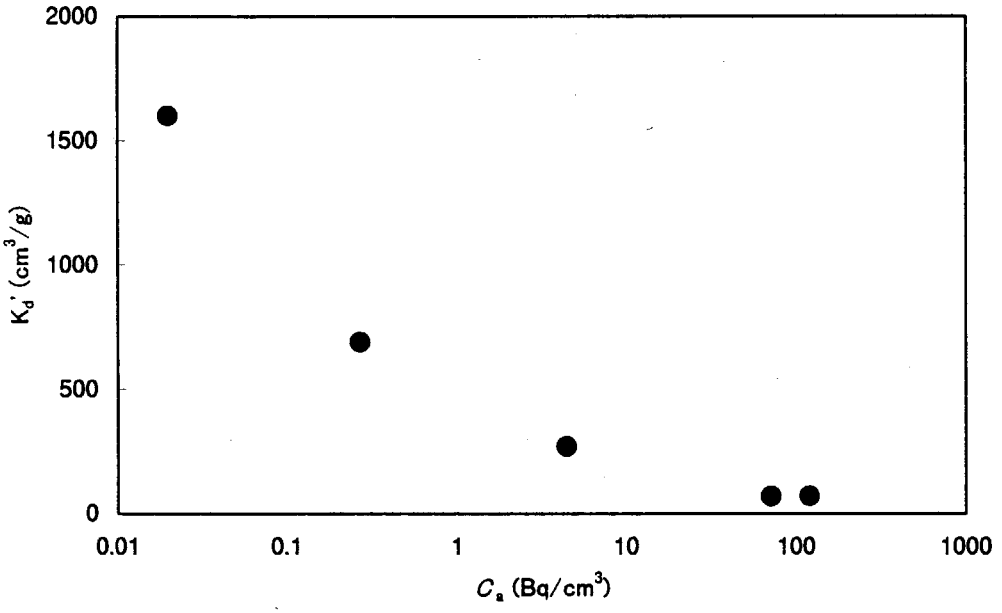

Fig.6 The relationship between ^{237}Np concentration in the solution C_a and apparent distribution coefficient K_d' corresponding to the ^{237}Np concentration; Relationship between ^{237}Np concentration and K_d' is given by $K_d' = 4 \times 10^2 C_a^{-0.42}$.

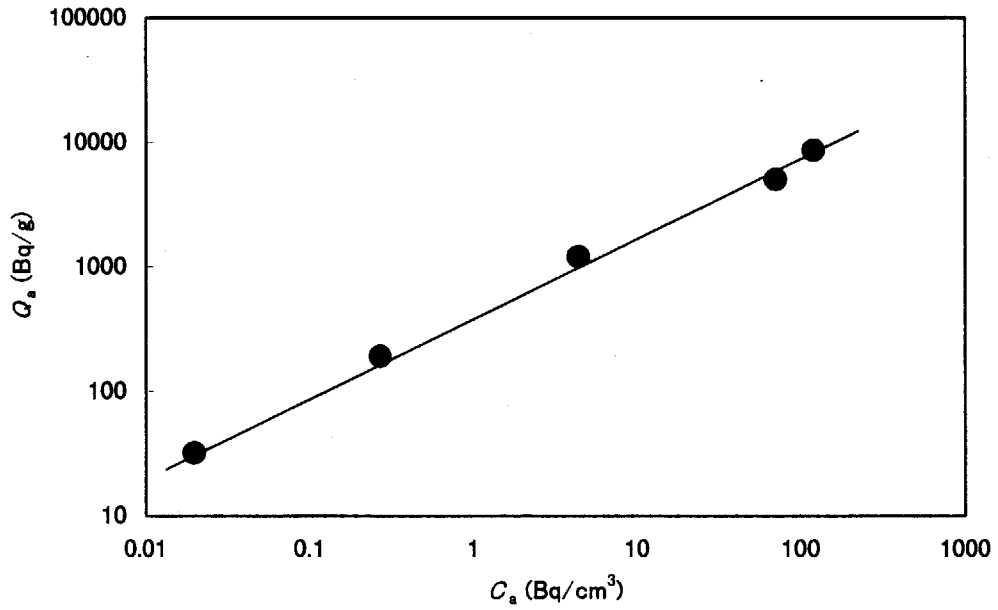

Fig.7 Adsorption isotherm of ^{237}Np on the loess; Plot of lnQ_a versus lnC_a was in a linear relation, where C_a is ^{237}Np concentration in the solution and Q_a is ^{237}Np concentration adsorbed on the loess. This result indicates that the adsorption isotherm of ^{237}Np is based on Freundlich's type.

国際単位系（SI）と換算表

表1 SI基本単位および補助単位

量	名称	記号
長さ	メートル	m
質量	キログラム	kg
時間	秒	s
電流	アンペア	A
熱力学温度	ケルビン	K
物質量	モル	mol
光度	カンデラ	cd
平面角	ラジアン	rad
立体角	ステラジアン	sr

表2 SIと併用される単位

名称	記号
分，時，日	min，h，d
度，分，秒	°，′，″
リットル	l，L
トン	t
電子ボルト	eV
原子質量単位	u

1 eV=1.60218×10^{-19}J

1 u=1.66054×10^{-27}kg

表5 SI接頭語

倍数	接頭語	記号
10^{18}	エクサ	E
10^{15}	ペタ	P
10^{12}	テラ	T
10^{9}	ギガ	G
10^{6}	メガ	M
10^{3}	キロ	k
10^{2}	ヘクト	h
10^{1}	デカ	da
10^{-1}	デシ	d
10^{-2}	センチ	c
10^{-3}	ミリ	m
10^{-6}	マイクロ	μ
10^{-9}	ナノ	n
10^{-12}	ピコ	p
10^{-15}	フェムト	f
10^{-18}	アト	a

表3 固有の名称をもつSI組立単位

量	名称	記号	他のSI単位による表現
周波数	ヘルツ	Hz	s^{-1}
力	ニュートン	N	$m\cdot kg/s^2$
圧力，応力	パスカル	Pa	N/m^2
エネルギー，仕事，熱量	ジュール	J	N·m
工率，放射束	ワット	W	J/s
電気量，電荷	クーロン	C	A·s
電位，電圧，起電力	ボルト	V	W/A
静電容量	ファラド	F	C/V
電気抵抗	オーム	Ω	V/A
コンダクタンス	ジーメンス	S	A/V
磁束	ウェーバ	Wb	V·s
磁束密度	テスラ	T	Wb/m^2
インダクタンス	ヘンリー	H	Wb/A
セルシウス温度	セルシウス度	℃	
光束	ルーメン	lm	cd·sr
照度	ルクス	lx	lm/m^2
放射能	ベクレル	Bq	s^{-1}
吸収線量	グレイ	Gy	J/kg
線量等量	シーベルト	Sv	J/kg

表4 SIと共に暫定的に維持される単位

名称	記号
オングストローム	Å
バーン	b
バール	bar
ガル	Gal
キュリー	Ci
レントゲン	R
ラド	rad
レム	rem

1 Å=0.1nm=10^{-10}m

1 b=100fm^2=10^{-28}m^2

1 bar=0.1MPa=10^{5}Pa

1 Gal=1cm/s^2=10^{-2}m/s^2

1 Ci=3.7×10^{10}Bq

1 R=2.58×10^{-4}C/kg

1 rad=1cGy=10^{-2}Gy

1 rem=1cSv=10^{-2}Sv

(注)

1．表1－5は「国際単位系」第5版，国際度量衡局1985年刊行による。ただし，1 eVおよび1 uの値はCODATAの1986年推奨値によった。

2．表4には海里，ノット，アール，ヘクタールも含まれているが日常の単位なのでここでは省略した。

3．barは，JISでは流体の圧力を表わす場合に限り表2のカテゴリーに分類されている。

4．EC閣僚理事会指令ではbar，barnおよび「血圧の単位」mmHgを表2のカテゴリーに入れている。

換算表

力	N(=10^{5}dyn)	kgf	lbf
	1	0.101972	0.224809
	9.80665	1	2.20462
	4.44822	0.453592	1

粘度　1 Pa·s(N·s/m^2)=10 P(ポアズ)(g/(cm·s))

動粘度　1 m^2/s=10^{4}St(ストークス)(cm^2/s)

圧力	MPa(=10bar)	kgf/cm^2	atm	mmHg(Torr)	lbf/in^2(psi)
	1	10.1972	9.86923	7.50062×10^3	145.038
	0.0980665	1	0.967841	735.559	14.2233
	0.101325	1.03323	1	760	14.6959
	1.33322×10^{-4}	1.35951×10^{-3}	1.31579×10^{-3}	1	1.93368×10^{-2}
	6.89476×10^{-3}	7.03070×10^{-2}	6.80460×10^{-2}	51.7149	1

エネルギー・仕事・熱量	J(=10^7 erg)	kgf·m	kW·h	cal(計量法)	Btu	ft·lbf	eV
	1	0.101972	2.77778×10^{-7}	0.238889	9.47813×10^{-4}	0.737562	6.24150×10^{18}
	9.80665	1	2.72407×10^{-6}	2.34270	9.29487×10^{-3}	7.23301	6.12082×10^{19}
	3.6×10^6	3.67098×10^5	1	8.59999×10^5	3412.13	2.65522×10^6	2.24694×10^{25}
	4.18605	0.426858	1.16279×10^{-6}	1	3.96759×10^{-3}	3.08747	2.61272×10^{19}
	1055.06	107.586	2.93072×10^{-4}	252.042	1	778.172	6.58515×10^{21}
	1.35582	0.138255	3.76616×10^{-7}	0.323890	1.28506×10^{-3}	1	8.46233×10^{18}
	1.60218×10^{-19}	1.63377×10^{-20}	4.45050×10^{-26}	3.82743×10^{-20}	1.51857×10^{-22}	1.18171×10^{-19}	1

1 cal= 4.18605J（計量法）

= 4.184J（熱化学）

= 4.1855J（15℃）

= 4.1868J（国際蒸気表）

仕事率　1 PS(仏馬力)

= 75 kgf·m/s

= 735.499W

放射能	Bq	Ci
	1	2.70270×10^{-11}
	3.7×10^{10}	1

吸収線量	Gy	rad
	1	100
	0.01	1

照射線量	C/kg	R
	1	3876
	2.58×10^{-4}	1

線量当量	Sv	rem
	1	100
	0.01	1

（86年12月26日現在）

Adsorption Mechanisms and Models of ^{85}Sr, ^{237}Np, ^{238}Pu and ^{241}Am in Loess Media (Joint Research)